THE JOURNAL OF BIOLOGICAL CHEMISTRY VOL. 282, NO. 5, pp. 2976–2986, February 2, 2007

Characterization of the Interactome of the Human MutL Homologues MLH1, PMS1, and PMS2*

Received for publication, October 24, 2006, and in revised form, December 4, 2006 Published, JBC Papers in Press, December 4, 2006, DOI 10.1074/jbc.M609989200

Elda Cannavo[‡], **Bertran Gerrits**[§], **Giancarlo Marra**[‡], **Ralph Schlapbach**[§], **and Josef Jiricny**[‡1]

From the [‡]*Institute of Molecular Cancer Research and the* [§]*Functional Genomics Center Zurich, University of Zurich, Winterthurerstrasse 190, CH-8057 Zurich, Switzerland*

Postreplicative mismatch repair (MMR) involves the concerted action of at least 20 polypeptides. Although the minimal human MMR system has recently been reconstituted *in vitro*, genetic evidence from different eukaryotic organisms suggests that some steps of the MMR process may be carried out by more than one protein. Moreover, MMR proteins are involved also in other pathways of DNA metabolism, but their exact role in these processes is unknown. In an attempt to gain novel insights into the function of MMR proteins in human cells, we searched for interacting partners of the MutL homologues MLH1 and PMS2 by tandem affinity purification and of PMS1 by large scale immunoprecipitation. In addition to proteins known to interact with the MutL homologues during MMR, mass spectrometric analyses identified a number of other polypeptides, some of which bound to the above proteins with very high affinity. Whereas some of these interactors may represent novel members of the mismatch repairosome, others appear to implicate the MutL homologues in biological processes ranging from intracellular transport through cell signaling to cell morphology, recombination, and ubiquitylation.

The postreplicative mismatch repair (MMR)[2] system maintains genomic stability by removing replication errors from DNA and by controlling the fidelity of recombination events, both mitotic and meiotic (1–4). Despite the fact that the human MMR pathway was recently reconstituted *in vitro* from purified individual components (5, 6), our knowledge of the molecular mechanisms of this process is still incomplete. The repair reaction requires a mismatch recognition step, which is mediated by the heterodimers of MSH2 (MutS homologue 2) and MSH6 (MutSα) or MSH2 and MSH3 (MutSβ). MutSα preferentially recognizes single base mismatches and small insertion-deletion loops (7, 8), whereas MutSβ recognizes preferentially larger insertion-deletion loops (9). Upon mismatch binding, the MutS (α or β) heterodimer associates with the heterodimeric complex of MLH1 (MutL homologue 1) and PMS2 (postmeiotic segregation 2) (MutLα) that was shown to be essential for repair (10). Until recently, the biochemical function of the MutL protein homologues remained enigmatic. MutLα was believed to couple the mismatch recognition step to downstream processes that include the removal of the mismatch from the nascent DNA strand, resynthesis of the degraded region, and ligation of the remaining nick (1, 11). MutLα was shown to possess a weak ATPase activity (12) that is essential for MMR, but the contribution of this enzymatic function to DNA metabolism was unclear. Most recently however, MutLα was shown to possess also an endonuclease activity, which introduces additional nicks into the discontinuous strand and thus facilitates the 5′ to 3′ degradation of the mismatch-containing strand by EXO1 (13, 14). This latter function helped explain why both EXO1, a 5′ to 3′ exonuclease, and MutLα, are required for 3′ to 5′ MMR. Moreover, characterization of the endonuclease activity of MutLα requires that the involvement of this heterodimer in biological processes other than MMR must be reexamined.

MLH1 can bind two other human MutL homologues, PMS1 and MLH3, to form the heterodimers MutLβ and MutLγ, respectively. *In vitro* studies failed to identify a role of MutLβ in MMR (15), whereas MutLγ can participate in the repair of base-base mismatches and small insertion-deletion loops, although its *in vivo* role seems to be only marginal (16). Interestingly, the active site of the MutLα endonuclease resides in the PMS2 subunit and is conserved in MLH3 but not in PMS1 (14). This explains why MutLα and MutLγ are active in MMR, whereas MutLβ is not.

MMR defects in humans are linked to hereditary nonpolyposis colon cancer, with *MLH1* mutations being responsible for ~60% of the cases. Animal models of the disease confirm this link; disruption of *Msh2* and *Mlh1* is associated with the most tumor-prone phenotype, whereas the severity of mutations in animals null for *Msh6*, *Pms2*, and *Mlh3* is reduced, which can be explained by the redundant roles played by the polypeptides encoded by the products of these genes in MMR. Correspondingly, mice lacking both MSH3 and MSH6 have a similar phenotype to animals deficient in MSH2, and those doubly mutant in MLH3 and PMS2 resemble MLH1-deficient mice (17–20). However, the biochemical roles of MMR proteins go beyond mismatch repair.

The mouse models confirmed the involvement of MMR proteins in mitotic recombination (19), since MLH1$^{-/-}$ (21) and MLH3$^{-/-}$ (22) knockout mice are not only cancer-prone but also sterile. Interestingly, in PMS2$^{-/-}$ animals, sterility is a fea-

* This work was supported in part by grants from the Swiss National Science Foundation, the European Union, and the Bonizzi-Theler Stiftung (to J. J.). The costs of publication of this article were defrayed in part by the payment of page charges. This article must therefore be hereby marked "*advertisement*" in accordance with 18 U.S.C. Section 1734 solely to indicate this fact.

[1] To whom correspondence should be addressed: Institute of Molecular Cancer Research, University of Zurich, Winterthurerstrasse 190, CH-8057 Zurich, Switzerland. Tel.: 41-44-6353450; Fax: 41-44-6353484; E-mail: jiricny@imcr.unizh.ch.

[2] The abbreviations used are: MMR, mismatch repair; HA, hemagglutinin; HA-Ubi, hemagglutinin-tagged ubiquitin; MNNG, *N*-methyl-*N*′-nitro-*N*-nitrosoguanidine; MS, mass spectrometry; TAP, tandem affinity purification; TEV, tobacco etch virus.

ture of male mice only (23), suggesting that PMS2 may have a more limited spectrum of meiotic functions than MLH1 and MLH3 (1, 24).

The importance of MMR proteins in DNA metabolism is further underscored by the findings that MMR status affects the outcome of other key processes, such as single strand annealing (25), class switch recombination, and somatic hypermutation of immunoglobulin genes (26), as well as triplet repeat expansions (27). Unfortunately, we currently lack mechanistic insights into these processes. In an attempt to elucidate the involvement of the MMR proteins in the above (and perhaps even in as yet unlinked) biological pathways, we set out to study the interactome of the human MutL homologues by tandem affinity purification (TAP). Several reports provide evidence that this technique, originally established in *Saccharomyces cerevisiae* (28, 29), represents a major improvement in the identification of protein-protein interactions. TAP represents a valuable method to identify interacting proteins *in vivo*, under native conditions and with a high degree of selectivity (30). We also carried out a large scale immunoprecipitation of PMS1 and analyzed the interacting partners of this third MutL homologue by mass spectrometry (MS). Our efforts led to the identification of a number of proteins complexed with MLH1, PMS1, or PMS2, some of which were described previously but the majority of which represented new interacting partners. It is hoped that further study of these interactions will help us uncover novel roles of the enigmatic MutL homologue family in human cells.

EXPERIMENTAL PROCEDURES

Plasmid Constructions—The mammalian vector for the expression of N-terminally TAP-tagged MLH1 was created by inserting the cDNA encoding the full-length MLH1 into the EcoRI site of pZome-1-N (Cellzome), and the vector for the expression of C-terminally TAP-tagged PMS2 was created by inserting the cDNA encoding the full-length PMS2 into the BamHI site of pZome-1-C (Cellzome). The vectors for the mammalian expression of Amot (angiomotin)/p80 and Amot/p130 were kindly provided by Dr. L. Holmgren (Karolinska Institute, Stockholm, Sweden). The pCDNA3-HA-Ubi vector, encoding HA-tagged ubiquitin, was kindly provided by Dr. D. Bohmann (School of Medicine and Dentistry, University of Rochester, Rochester, NY).

Cell Culture and Transfections—The human 293, 293T, and HeLa cells were obtained from the cell line repository of Cancer Network Zurich, and the HeLa12 cell line was kindly provided by Dr. M. Bignami (ISS, Rome, Italy). All of the cell lines were cultured at 37 °C in a 5% CO_2 humidified atmosphere and maintained in the appropriate media. Transfection was performed using the Fugene 6 transfection reagent (Roche Applied Science) according to the manufacturer's recommendations. For generation of stable cell lines, 0.2 μg/ml puromycin (Invivogen) was added to the medium 1 day after transfection. After 2 weeks, the surviving colonies were isolated and their extracts were screened by Western blot using antibodies against MLH1 and PMS2. The clones showing the highest expression of the two tagged mismatch repair proteins were further subcloned.

Western Blot Analyses and Antibodies—Preparation of whole cell extracts and Western blot analyses were performed as described previously (31) using the following antibodies: MLH1 and PMS2 from BD PharMingen (1:4000 and 1:1000, respectively), β-tubulin and BRCA1 (breast cancer-associated protein-1) from Santa Cruz Biotechnology, Inc. (Santa Cruz, CA) (1:2000 and 1:500, respectively), BRIP1 (BRCA1 interacting protein C-terminal helicase 1) from Novus Biologicals (1:4000), MSH6 from Transduction Laboratories (1:1000), and ubiquitin from BAbCO (1:1000). The anti-angiomotin antibody was a kind gift of Dr. L. Holmgren (Karolinska Institute, Stockholm, Sweden). For the immunoprecipitation experiment, the anti-PMS1 rabbit polyclonal antibody (15) was further affinity-purified. Briefly, 10 mg of purified His_6-tagged internal peptide of PMS1 (amino acids 335–643) were coupled to 0.4 g of CNBr-activated Sepharose 4B (Amersham Biosciences), according to the manufacturer's instructions. 5 ml of rabbit polyclonal anti-PMS1 serum diluted 10× in 50 mM Tris-HCl, pH 7.5, was then bound to the CNBr-bound antigen for 4 h at 4 °C. After two washes in 10 mM Tris-HCl, pH 7.5, and two additional washes in 10 mM Tris-HCl, pH 7.5, 500 mM NaCl, the antibody was eluted with 100 mM glycine-HCl, pH 2.5, at 4 °C. The elution step was repeated twice, and the final eluates were pooled in new tubes containing 1 M Tris-HCl, pH 8.0, to a final concentration of 100 mM. 300 μl of the corresponding preimmune serum were IgG/A-purified by binding to 300 μl of Protein A/G Plus-agarose (Santa Cruz Biotechnology). Elution of the IgG/A bound antibodies was then performed as above.

Co-immunoprecipitations—Co-immunoprecipitations were performed as described previously (16). Control experiments were done in the absence of the primary antibody. The detection of PMS1 polyubiquitylation was carried out as described (32).

Testing of MMR Status—In vitro MMR assays, the *N*-methyl-*N*′-nitro-*N*-nitrosoguanidine (MNNG) sensitivity assay, and fluorescence-activated cell sorting analyses were performed as described previously (31).

TAP—293T and HeLa12 cells stably transfected with plasmids expressing the N-terminally TAP-tagged MLH1 and the C-terminally TAP-tagged PMS2 (TAP-MLH1/293T and TAP-PMS2/HeLa12 cell lines, respectively) were plated in 15-cm dishes. Cells were cultured to 80% confluence, washed twice in cold PBS, and lysed for 30 min on ice in 50 mM Tris-HCl, pH 8.0, 125 mM NaCl, 1% Nonidet P-40, 2 mM EDTA, 1 mM phenylmethylsulfonyl fluoride, 1× complete inhibitory mixture (Roche Applied Sciences), 0.5 mM sodium orthovanadate, 20 mM sodium fluoride, and 5 nM okadaic acid. The lysates were cleared by centrifugation at 12,000 × *g* for 3 min, and the soluble material was collected. Protein concentrations were determined using the Bradford assay (Bio-Rad).

Tandem affinity purification was performed batchwise according to the original protocol (29) with minor changes. All of the following purification steps were performed on ice or at 4 °C. For each experiment, 60 mg of whole cell extract were incubated for 4 h with gentle agitation with 100 μl of IgG-Sepharose beads (Amersham Biosciences) equilibrated with lysis buffer. Beads were then washed three times with 1 ml of lysis buffer and three times with 1 ml of tobacco etch virus

(TEV) buffer (10 mM Hepes-KOH, pH 8.0, 150 mM NaCl, 0.1% Nonidet P-40, 0.5 mM EDTA, 1 mM dithiothreitol, 1 mM phenylmethylsulfonyl fluoride, and 1× complete inhibitory mixture). Bound TAP-tagged proteins were released by overnight incubation in TEV buffer containing 16 units of acTEV protease (Invitrogen) in tubes mounted on a rotating platform. The supernatant from the TEV reaction was collected and transferred to a new tube. One volume of calmodulin binding buffer (10 mM β-mercaptoethanol, 10 mM Hepes-KOH, pH 8.0, 150 mM NaCl, 1 mM MgOAc, 1 mM imidazole, 0.1% Nonidet P-40, 2 mM $CaCl_2$, 1 mM phenylmethylsulfonyl fluoride, and 1× complete inhibitory mixture) was added to the collected supernatant and centrifuged at 1500 rpm for 3 min in an Eppendorf centrifuge. The supernatant was then transferred to a new tube, and the procedure described above was repeated two more times. 1/250 volume of 1 M $CaCl_2$ was then added, and the supernatant was batch-purified by binding to 100 μl of calmodulin affinity resin (Stratagene) equilibrated in calmodulin binding buffer for 4 h on a rotating platform. Beads were washed three times with 1.2 ml of calmodulin binding buffer and twice with 1.2 ml of calmodulin rinsing buffer (50 mM ammonium bicarbonate, pH 8.0, 75 mM NaCl, 1 mM MgOAc, 1 mM imidazole, and 2 mM $CaCl_2$) and eluted with 100 μl of calmodulin elution buffer (50 mM ammonium bicarbonate, pH 8.0, and 35 mM EGTA). One-third of the eluate was separated by SDS-PAGE and visualized by silver staining. As negative control, the purification was performed with extracts prepared from parental cells not expressing the tagged protein.

Liquid Chromatography-MS/MS Analysis—The eluate from two TAP experiments (total volume 200 μl) was concentrated using the Microcon YM-3 concentrator (Millipore) according to the manufacturer's instructions, separated by 7.5% SDS-PAGE and visualized by Coomassie staining. The gel was then cut into 11 slices, and the polypeptides were subjected to in-gel tryptic digest. Briefly, the gel slices were cut into small fragments and subjected to two cycles of rehydration in 50 mM ammonium bicarbonate and shrinking by dehydration in 80% acetonitrile. The proteins were then reduced with 37 mM dithiothreitol in 50 mM ammonium bicarbonate at 50 °C for 30 min. After two rounds of dehydration, the proteins were alkylated with 20 mM iodoacetamide in 50 mM ammonium bicarbonate for 15 min at room temperature in the dark. After three further rounds of rehydration and shrinking, the gel pieces were incubated with 200 ng of sequencing grade modified trypsin (Promega) for 4 h at 37 °C and then at 25 °C overnight. The peptides were extracted by one change of 0.1% formic acid and three changes of 80% acetonitrile, 0.1% formic acid and dried under vacuum. The tryptic peptides were analyzed on an LTQ-FT™ analyzer (Thermo Electron, Bremen, Germany). Peptides were separated on a nano-high pressure liquid chromatograph (Agilent, Palo Alto, CA) online prior to MS analysis on a C_{18} reversed phase column (Magic 5-μm 100-Å C_{18} AQ; Michrom, Auburn, CA), using an acetonitrile/water system at a flow rate of 200 nl/min. Tandem mass spectra were acquired in a data-dependent manner. Typically, four MS/MS were performed after each high accuracy spectral acquisition range survey. The human portion (taxonomy ID: 9606) of the UniProt data base (available on the Internet at ftp.ebi.ac.uk/pub/databases/SP proteomes/fasta/proteomes/25.H_sapiensfasta.gz) was interrogated using the Mascot search algorithm (33). One failed trypsin cleavage was allowed per search. The precursor and fragment ion tolerances were set to 5 ppm and 0.8 Da, respectively.

RESULTS

Generation and Characterization of Stable Mammalian Cell Lines Expressing TAP-tagged MLH1 and PMS2—TAP was shown to be a powerful method for identification of interacting partners of known proteins in various host cell lines (29, 30). In order to avoid competition, it is preferable to use cell lines lacking the corresponding endogenous protein. For this reason, we stably transfected two human cell lines deficient for MLH1 or PMS2, namely the MLH1-deficient embryonic kidney cell line 293T (34) and the PMS2-deficient ovarian carcinoma cell line HeLa12 (35) with pZome-1-N-MLH1 and pZome-1-C-PMS2, respectively. The resulting clones were analyzed by Western blot for the expression of the TAP-tagged protein MLH1 or PMS2 (see "Experimental Procedures" for details). Since the stable clones exhibited different expression levels of the transfected proteins (data not shown), we selected two that expressed the TAP-tagged proteins at levels comparable with those present in the MMR-proficient cell line HeLa (Fig. 1*A*). The TAP-tagged proteins translocated in both cases into the nucleus as ascertained by indirect immunofluorescence or immunohistochemistry (data not shown).

To rule out the possibility that the TAP tag impairs the function of MLH1 or PMS2, we performed *in vitro* MMR assays with cytoplasmic extracts from TAP-MLH1/293T and TAP-PMS2/HeLa12 cells. As shown in Fig. 1*B*, the MMR activity in both cell lines was comparable with the repair activity of MMR-proficient HeLa cells.

Treatment of mammalian cells with low doses of S_N1 type alkylating agents, such as MNNG, induces a G_2 cell cycle arrest that is absolutely dependent on functional MMR (36). We confirmed this hallmark of MMR proficient cells in our stable cell lines by fluorescence-activated cell sorting analysis. Both TAP-MLH1/293T and TAP-PMS2/HeLa 12 cell lines arrested in the G_2 phase of the cell cycle upon treatment with 0.2 μM MNNG for 24 h (Fig. 1*C*). The arrest of cell growth upon treatment with MNNG was also confirmed by clonogenic assays (data not shown). In summary, the TAP tag impairs the function of neither MLH1 nor PMS2 in MMR.

Tandem Affinity Purifications—Since its first description in 1999 (28), TAP tagging has been successfully used in the identification of binding partners of various proteins (29, 30). The affinity tag consists of two IgG binding domains of the *Staphylococcus aureus* protein A and of a calmodulin binding peptide, whereby the two motifs are separated by a TEV protease cleavage site. We placed the TAP tag at the N terminus of MLH1, since the C terminus of this polypeptide is extremely sensitive to modification (37), and at the C terminus of PMS2 (Fig. 2*A*). The protein complexes were then isolated by chromatography on IgG-Sepharose, followed by elution with TEV protease and loading onto calmodulin-Sepharose. The final elution was carried out with EGTA (Fig. 2*B*). TAP and liquid chromatography-MS/MS analysis (Fig.

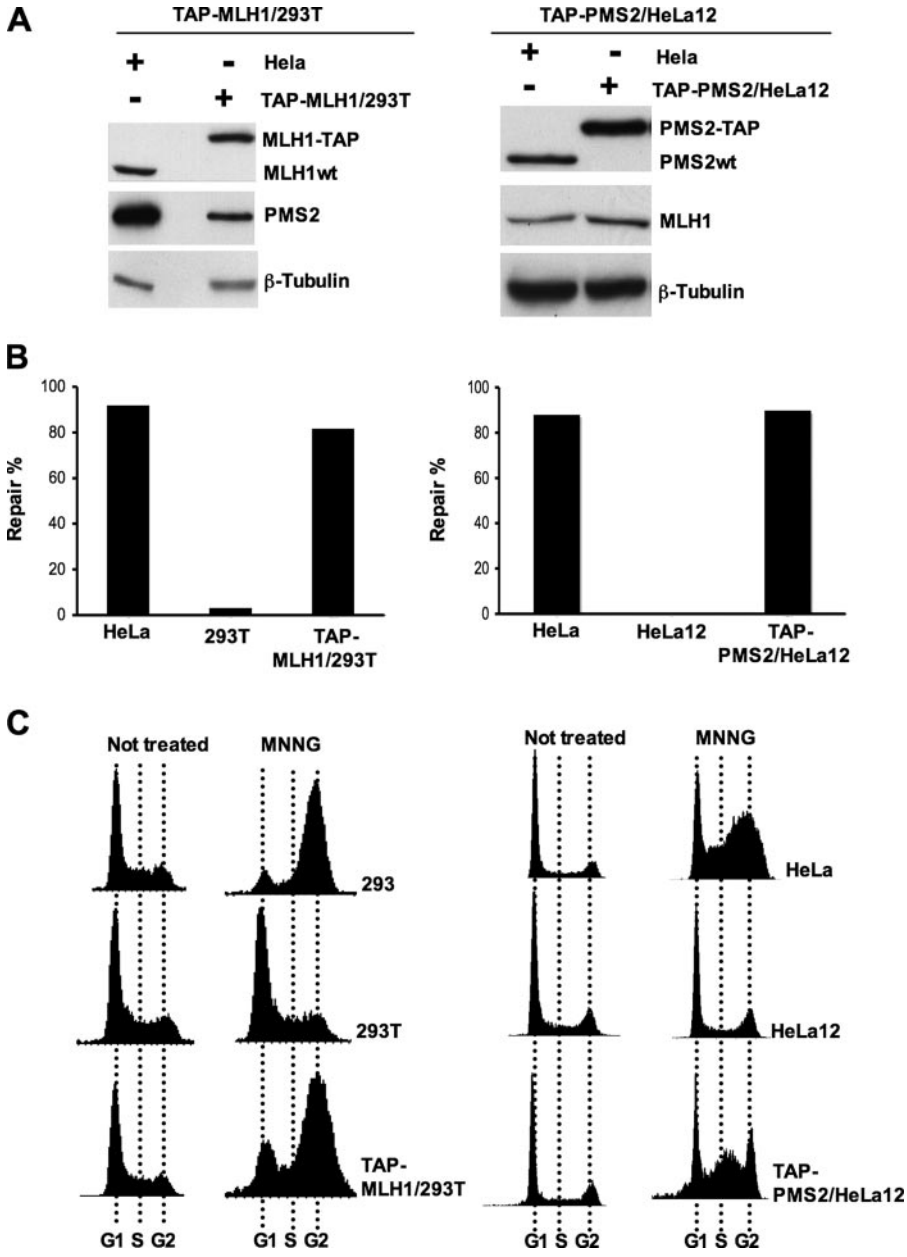

FIGURE 1. **Characterization of mammalian cell lines stably expressing TAP-tagged MLH1 and PMS2.** *A*, whole cell extracts of TAP-MLH1/293T (*left*) and TAP-PMS2/HeLa12 cells (*right*) were analyzed by Western blot (50 μg of extract/lane) for the expression of MLH1 and PMS2. In both cell lines, the expression of the TAP-tagged proteins was roughly comparable with the amounts of these proteins in 50 μg of whole cell extract from the MMR-proficient cell line HeLa (*left*). Note that TAP-MLH1 and TAP-PMS2 migrate slower due to the presence of the TAP tag. *B*, *in vitro* MMR assays. The repair efficiency of the extracts of TAP-MLH1/293T (*left*) and TAP-PMS2/HeLa12 (*right*) cells was compared with the repair efficiency of the extracts from corresponding parental MMR-deficient cell lines 293T or HeLa12, respectively. The repair efficiencies were determined on hetroduplex substrates containing a G/T mismatch (for details, see "Experimental Procedures"). Extracts from the MMR-proficient HeLa cells were used as a positive control. *C*, FACS profiles of the MMR-proficient or -deficient 293 and 293T cells (*left*) and HeLa or HeLa12 cells (*right*) were compared with the profiles of TAP-MLH1/293T (*left*) and TAP-PMS2/HeLa12 (*right*) cells either untreated or treated with 0.2 μM MNNG for 24 h. The figure shows that expression of the TAP-tagged variants of MLH1 and PMS2 restored MMR proficiency and cell cycle checkpoint activation to the MMR-deficient cell lines 293T and HeLa12.

2*C*) were performed as described under "Experimental Procedures." Each experiment was repeated several times, and the results were highly reproducible, as judged by comparing silver-stained gels from independent experiments (data not shown).

Identification of Interacting Partners of MLH1 and PMS2—Each TAP experiment was performed with 2 × 60 mg of whole cell extracts. Upon concentration, the final eluate was subjected to electrophoresis on SDS-PAGE, and the protein bands were visualized by silver staining for analytical purposes and by Coomassie Blue staining for MS analysis. The bait protein and its partner(s) were detected as the most prominent bands, migrating at the predicted molecular sizes (Fig. 3*A*). The identity of these bands was also independently confirmed by Western blotting (Fig. 3*B*). The lanes containing the TAP eluates were then cut into 11 slices, and the proteins in each slice were identified by MS analysis of their tryptic peptides. As anticipated, the highest Mascot scores belonged to MLH1, PMS1, and PMS2, but we were able to identify also a large number of other proteins in the TAP-MLH1 or TAP-PMS2 eluates. First, we verified that the detected proteins were isolated from the gel area corresponding to their predicted molecular sizes. Next, we classified the proteins into several groups according to the known function. A selection of MLH1 and PMS2 interactors are listed in Tables 1 and 2, respectively.

In the MLH1-TAP experiment, one of the most prominent polypeptides was PMS1 (Fig. 3, *A* (*left*) and *C*), which interacts *in vivo* with MLH1 to form the heterodimer MutLβ (15). As noted above, PMS1 lacks the endonuclease active site conserved in PMS2 and MLH3 (14), and mice lacking this polypeptide are not cancer-prone (17). The biological roles of PMS1 and MutLβ thus remain enigmatic. As anticipated, we found PMS1 associated with MLH1 in the TAP eluate from the cell line expressing TAP-tagged MLH1, but not TAP-tagged PMS2 (Fig. 3*A*) (Tables 1 and 2), which confirms that PMS2 and PMS1 compete for MLH1 (15, 37). Given that the intracellular level of PMS1 was reported to be lower than that of PMS2 (15), the fact that these two proteins were pulled down in similar amounts shows that the affinity of MLH1 for PMS1 is high.

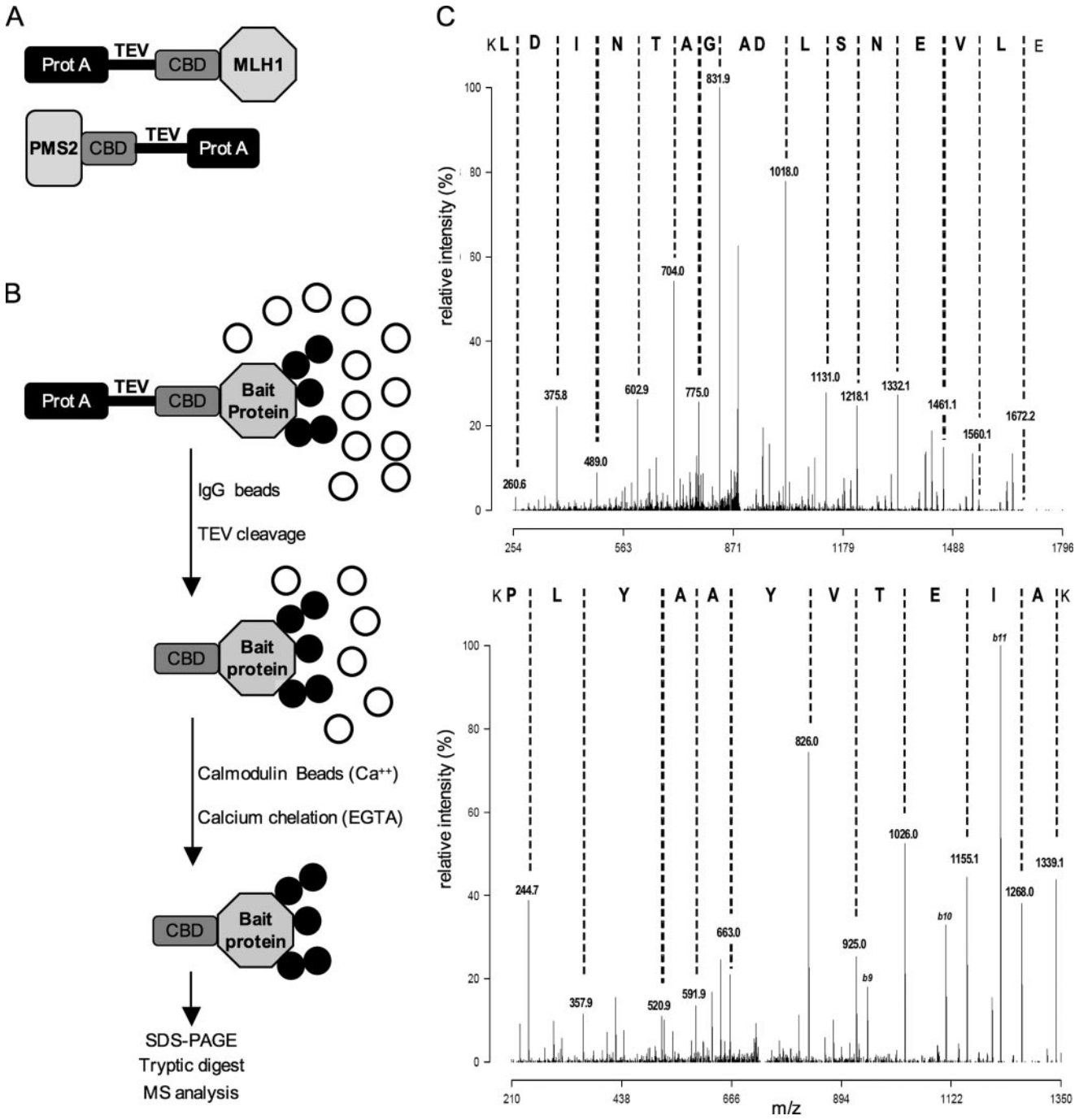

FIGURE 2. **Tandem affinity purifications.** *A*, schematic representation of the MLH1-TAP (*top*) and PMS2-TAP (*bottom*) constructs. The TAP tag was inserted at the N terminus of MLH1 and at the C terminus of PMS2. *Prot A*, Protein A (IgG binding) domain; *TEV*, TEV protease cleavage site; *CBD*, calmodulin binding domain. *B*, overview of the purification procedure. *Black circles*, factors that specifically interact with the bait protein; *white circles*, noninteractors (see"Results" for details). *C*, tandem mass spectra of tryptic peptides from PMS2 and MLH1 identified in the TAP of MLH1 and PMS2, respectively. For clarity, only the y-ion series are labeled in both panels. The *top* shows the MS/MS spectrum of $[M + 2H]^{2+} = 901.4644$, which was identified as the peptide ELVENSLDAFATNIDLK from PMS2 found in the TAP of MLH1. The peptide was identified with a Mascot score of 104, whereas the overall protein coverage was 59% with a score of 4117. The *bottom* shows the MS/MS spectrum of $[M + 2H]^{2+} = 733.9164$. The peptide identified was KAIETVYAALPK from MLH1 found in the TAP of PMS2, with a peptide ion score of 97. The overall protein coverage was 85% with a Mascot score of 4158.

The interaction of MLH1 with MLH3, which forms the third MLH1-containing heterodimer, MutLγ, could not be confirmed, because the *MLH3* gene in the 293T cell line is transcriptionally silenced by promoter methylation (16).

Our analysis (Tables 1–3) identified also several other previously described interactors. The 5′–3′ exonuclease EXO1, which was shown to interact with MutLα in co-immunoprecipitation and pull-down experiments (38, 39), was present in both MLH1-TAP and PMS2-TAP fractions. Proliferating cell nuclear antigen was shown to interact with MLH1 in yeast two-hybrid and co-immunoprecipitation experiments (40, 41). Although we did not identify proliferating cell nuclear antigen peptides in the eluate from TAP-MLH1 with a significant score, the protein was present at significant levels in the complex

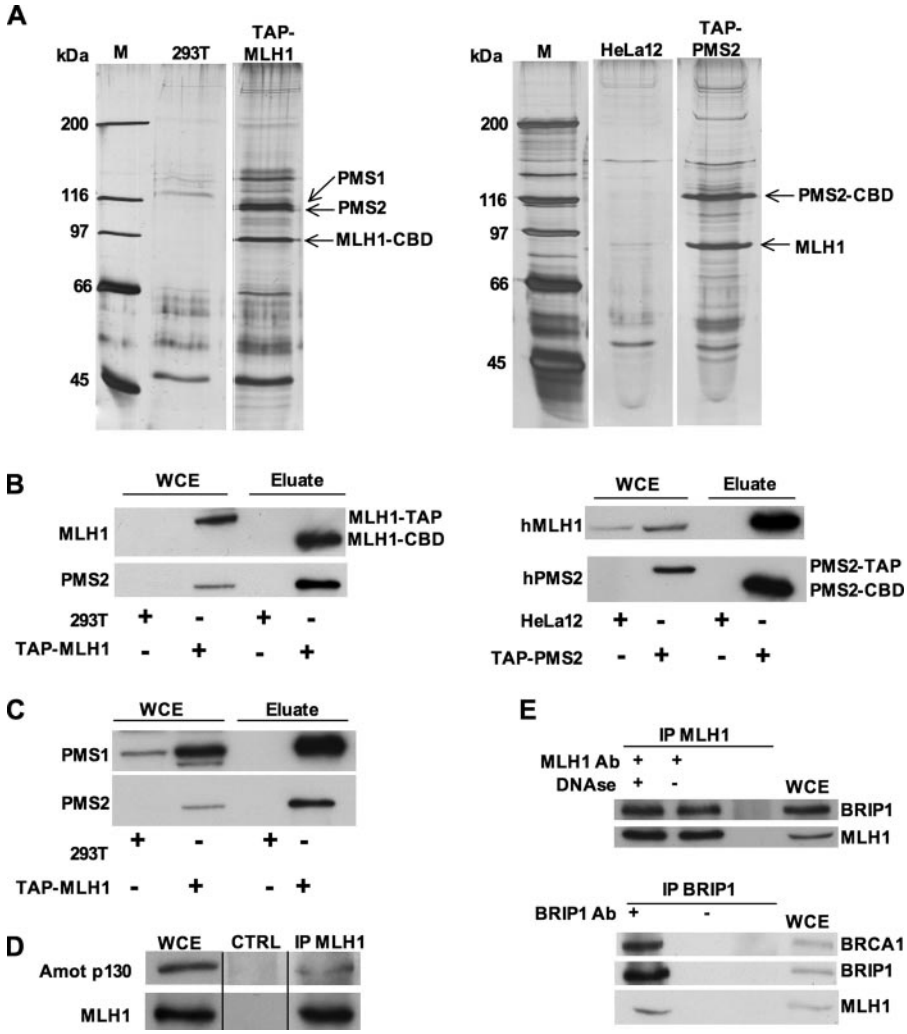

FIGURE 3. **Analysis of MLH1- and PMS2-interacting partners by TAP.** *A*, analysis of the TAP-MLH1 (*left panel*, *right lane*) and TAP-PMS2 (*right panel*, *right lane*) interactomes. TAP with extracts from corresponding parental untransfected cells (*middle lanes*) were used as negative controls. One-third of the final eluate from 60 mg of whole cell extract (see "Experimental Procedures" for details) was resolved on SDS-PAGE and visualized by silver staining. The bands corresponding to the tagged protein and its major *in vivo* interactor(s) are indicated. *M*, molecular size marker; *CBD*, calmodulin binding domain. *B*, Western blot analyses. 50 μg of whole cell extract (*WCE*) or 33 μl of TAP eluate were loaded on SDS-PAGE and analyzed by Western blot using specific antibodies against human MLH1 and PMS2. Extracts and eluates from parental untransfected cell lines 293T (*left panel*) and HeLa12 (*right panel*) were compared with samples from the stable cell lines TAP-MLH1/293T (*left*) and TAP-PMS2/HeLa12 (*right*). Note that the TAP-tagged MLH1 and PMS2 migrate slower due to the presence of the TAP tag or of the CBD. *C*, relative abundance of PMS1 and PMS2 in TAP eluates. 50 μg of whole cell extract from 293T and TAP-MLH1/293T cells or 33 μl of the final eluate from the TAP-MLH1 were loaded on SDS-PAGE and analyzed by Western blot using specific antibodies against human PMS1 and PMS2. *D*, 293 cells were transiently transfected with the cDNA encoding Amot/p130. One mg of whole cell extract from the transfected cells was incubated with (*IP MLH1*) or without (*CTRL*) the anti-MLH1 antibody. *E*, co-immunoprecipitation of MLH1 and BRIP1 in HeLa cells. 500 μg of whole cell extract were incubated with or without anti-MLH1 antibody (*top*) or anti-BRIP1 antibody (*bottom*). *DNase*, extract treated with DNase prior to IP. This experiment shows that the interaction between BRIP1 and MLH1 is not mediated by DNA. This reaction was carried out in the presence of 25 units of benzonase.

bound to PMS2. In addition to EXO1 and proliferating cell nuclear antigen, we could detect other proteins involved in MMR, including MSH2, MSH6, and replication factor C, among the PMS2-bound proteins. Thus, with the notable exception of DNA polymerase δ and replication protein A, factors required for the recently reconstituted MMR reaction *in vitro* (5) were specifically detected in the TAP eluates.

MLH1 was also described to associate with the breast cancer susceptibility gene product BRCA1 in the so-called BASC complex (42). The same group later described the binding of BRCA1 to SMC1 (structural maintenance of chromosome protein 1) upon DNA damage (43). The finding of both proteins, BRCA1 and SMC1, in our TAP-MLH1 eluate is a further validation of our experimental conditions.

Although many interactions between our bait proteins and their known interacting factors could be confirmed with our TAP strategy, this was not always the case. For instance, we failed to detect interactions between MLH1 and the Bloom's helicase (44), MRE11 (45), or MBD4 (methyl-CpG binding domain protein 4) (MED1) (46). This could be explained by the differences between the TAP protocol and the experimental systems deployed in the latter studies. Moreover, we cannot exclude the possibility that the presence of the TAP tag on our bait proteins interfered with the binding of these polypeptides.

The primary focus of this study was to detect novel interacting partners of the human MutL homologues, in an attempt to explain the involvement of these proteins in MMR and other biological processes. As shown in Tables 1 and 2, the TAP approach succeeded in identifying numerous novel partners of both MLH1 and PMS2. For example, MLH1 appears to be in a stable complex with Amot (Table 1). This polypeptide was identified during a search for angiostatin interactors in a yeast two-hybrid assay (47). We were initially skeptical about this assignment for two reasons. First, the 80-kDa Amot was reported to be involved in the control of migration of endothelial cells, and second, our MS analysis identified Amot in an SDS-PAGE band that was expected to contain proteins in the 120–130-kDa range. Interestingly, a few weeks after we identified Amot as an MLH1-interacting protein, an alternatively spliced isoform of Amot, which has a molecular size of 130 kDa, was described (48, 49). It appears to localize to cell-cell junctions and affect endothelial cell shape (48). We confirmed the specificity of the interaction between MLH1 and angiomotin p130 by co-immunoprecipitation (Fig. 3*D*).

It is known that both MLH1 and PMS2 contain a monopartite nuclear localization signal and that certain mutations within this nuclear localization signal impair their nuclear

TABLE 1

The TAP interactome of MLH1

The table lists a selection of proteins identified in the MLH1-TAP eluate. The full list is available upon request.

Function/Protein[a]	Protein score[b]	Coverage	Swiss-Prot accession number
		%	
Mismatch repair			
MLH1	7390	70	P40692
PMS1	7143	70	P54277
PMS2	4117	59	P54278
MSH3	628	22	P20585
Exonuclease 1	72	6	Q5T396
DNA metabolism/repair			
DNA-PKcs	483	9	P78527
BRCA1	202	11	Q5YLB2
SMC1A	68	10	Q14683
SEP1 (XRN1)	330	9	Q8IZH2
Protein import/export			
Importin α2	336	18	P52292
Importin β1	118	3	Q14974
Ubiquitin pathway/proteasome			
PSD3	243	18	O43242
UBP2L	183	12	Q14157
Ubiquitin	172	45	P62988
DNA helicases			
BRIP1 (BACH1)	3905	53	Q9BX63
RuvB-like 1	309	22	Q9Y265
RuvB-like 2	76	8	Q9Y230
Unknown function/hypothetical proteins			
KIAA1018 (fragment)	898	27	Q9Y2M0
YLPM1 (ZAP3)	184	3	P49750
Cell cycle/signaling/kinases/phospatases/apoptosis			
PP2A regulatory subunit A-α	278	19	P30153
PP2A regulatory subunit B-α	152	10	P63151
PP2A regulatory subunit B-β	99	6	Q00005
P2BB catalytic subunit β	184	19	P16298
P2BC catalytic subunit γ	122	10	P48454
PP2A regulatory subunit B-δ	99	8	Q6IN90
PDCD8	169	15	O95831
PI3K-C2α	160	6	O00443
Others			
Angiomotin	4013	57	Q4VCS5
ATAD3A	470	25	Q9NVI7
DOCK7	460	9	Q5T1C0
PYGB	269	10	P11216
ATPα	953	39	P25705
ATAD3B	244	19	Q5T9A4
REC14 (WDR61)	155	7	Q6IA22

[a] Derived from the Swiss-Prot data base or published data.
[b] Mascot protein score of >65 was considered significant ($p < 0.05$).

TABLE 2

The TAP interactome of PMS2

The table lists a selection of proteins identified in the PMS2-TAP eluate. The full list is available upon request.

Function/Protein[a]	Protein score[b]	Sequence coverage	Swiss-Prot accession number
		%	
Mismatch repair			
MLH1	4158	85	P40692
PMS2	3601	71	P54278
MSH2	1529	31	P43246
MSH3	993	24	P20585
MSH6	108	4	P52701
Exonuclease 1	164	12	Q5T396
PCNA	184	15	P12004
RFC 40 kDa	82	10	P35250
DNA metabolism/repair			
DNA-PKcs	1938	13	P78527
BRCA2	114	8	P51587
DDB1	114	8	Q16531
MMS19-like	97	5	Q5T455
CAD (PYR1)	1718	19	P27708
MCM3	130	7	P25205
BRG1 (SMCA4, SMARCA4)	280	5	P51532
Protein import/export			
Importin α2	535	22	P52292
Importin β1	425	12	Q14974
CRM1 (XPO1)	797	17	O14980
COPB	741	24	P53618
COPG	170	4	Q9Y678
COPG2	112	7	Q9UBF2
Ubiquitin pathway/proteasome			
PSD2	818	24	Q13200
PRS4	378	29	P62191
PRS10	253	14	P62333
PSD5	245	16	Q16401
PSD3	234	14	O43242
PRS6A	132	12	P17980
PRS7	108	7	P35998
Ubiquitin	127	45	P62988
CYLD	241	10	Q9NQC7
EDD	206	8	O95071
DNA helicases			
BRIP1 (BACH1)	720	14	Q9BX63
RuvB-like 1	710	33	Q9Y265
RuvB-like 2	570	24	Q9Y230
Unknown function/hypothetical proteins			
KIAA1018 (fragment)	454	14	Q9Y2M0
DKFZp686L22104	103	21	Q68E03
Cell cycle/signaling/kinases/phospatases/apoptosis			
PP2A catalytic subunit α	131	12	P67775
PDCD8	90	6	O95831
PI3K-C2α	67	9	O00443
Others			
ATAD3A	571	30	Q9NVI7
NSUN2	145	10	Q9BVN4

[a] Derived from the Swiss-Prot data base or published data.
[b] Mascot protein score of >65 was considered significant ($p < 0.05$).

import (50, 51). Nuclear localization signals are recognized by specialized transport factors, karyopherins or importins, which function as heterodimeric protein complexes that dock to nuclear localization signal-containing substrates and mediate their import into the nucleus (52). We identified importin α2 and its known binding partner importin β1 in the complex with both MLH1 and PMS2 (Tables 1 and 2). This finding suggests that the importin α2/β1 heterodimer might be the nuclear transporter of human MutLα.

Of particular interest is the identification of BRCA1-associated C-terminal helicase BRIP1 (also known as BACH1), in the MLH1- and PMS2-bound complexes (Tables 1 and 2). BRIP1/BACH1 was recently identified as the Fanconi anemia J protein (53–55) and appears to be critical for homologous recombination, DNA double strand break repair, and interstrand cross-link repair (55, 56). We confirmed the binding of BRIP1 to MLH1 by reciprocal immunoprecipitation and Western blot (Fig. 3*E*). BRCA1 was also present in the complex.

As mentioned above, the interaction between BRCA1 and MLH1 had been described earlier (42) and could be confirmed in the present study. However, the low protein score for BRCA1 (Table 1) suggested either that the interaction was only weak or, alternatively, that BRCA1 was bound to MLH1 indirectly, possibly via BRIP1. The same could apply also to BRG1/SMARCA4/SMCA4 (Table 2). This polypeptide has been reported to interact with BRCA1 and is believed to act as a cofactor of c-Myc in oncogenic transformation (57). It has a DNA-dependent ATPase activity, which may be required for

TABLE 3

Proteins co-immunoprecipitating with PMS1

The table lists a selection of proteins identified in a co-immunoprecipitate with PMS1. The full list is available upon request.

Function/Protein[a]	Protein score[b]	Sequence coverage	Swiss-Prot accession number
		%	
Mismatch repair			
MLH1	3692	74	P40692
PMS1	3118	70	P54277
RFC 40 kDa	120	18	P35250
RFC 37 kDa	111	11	P35249
RFC 140 kDa	98	6	P35251
Exonuclease 1	65	10	Q5T396
RPA 40 kDa	83	12	O15160
DNA metabolism/repair			
BRCA2	224	10	P51587
MMS19-like	103	14	Q5T455
ATR	157	9	Q13535
NONO	283	28	Q9BQC5
PGK1	487	30	P00558
TOP1	403	18	P11387
MCM6	278	12	Q14566
DPOZ	229	8	O60673
SMC3	170	17	Q9UQE7
Protein import/export			
Importin β3	851	24	O00410
Importin α2	312	23	P52292
Importin 9	296	11	Q96P70
RANBP9	338	20	Q96S59
RANGAP1	243	29	Q96JJ2
Ubiquitin pathway/proteasome			
EDD	2558	34	O95071
UBP5	963	35	P45974
CYLD	183	7	Q9NQC7
UBP13	141	15	Q92995
Ubiquitin	111	58	P62988
RNF123	103	7	Q5XPI4
UBAP2L	101	7	Q9BTU3
PSD2	506	23	Q13200
PRS4	198	16	P62191
Herc2	213	8	O95714
Cullin 3	190	15	Q13618
Cullin 1	134	11	Q13616
USP9Y	102	6	O00507
RNF20	188	14	Q5VTR2
DNA helicases			
DNA helicase B	706	23	Q8NG08
MOV10	330	14	Q9HCE1
BRIP1	159	15	Q9BX63
Cell cycle/signaling/kinases/ phospatases/apoptosis			
SET binding factor 2	759	17	Q86WG5
SET binding factor 1	194	8	O95248
Cyclin T1	483	30	O60563
CDK9	444	38	P50750
PI3K-C2α	443	15	O00443
CDC5-like	338	22	Q76N46
AKAP9	323	15	Q99996
PP2A regulatory subunit A-α	263	22	P30153

[a] Derived from the Swiss-Prot data base or published data.
[b] Mascot protein score of >65 was considered significant ($p < 0.05$).

transcriptional activation of certain genes (58) as part of a SWI/SNF chromatin remodeling complex (59). This latter complex contains also two proteins related to the bacterial ATP-dependent helicase RuvB: RuvBL1 (TIP49a) and RuvBL2 (TIP49b), which were identified in association with both MLH1 and PMS2. RuvBL1 and RuvBL2 are highly conserved in evolution and are essential for viability in yeast. The precise role of these ATPase-helicases is not known, but they were reported to be associated with transcription factors (60, 61) and to modulate apoptosis (62) and oncogenic transformation (63, 64), and they were shown to be in chromatin remodeling complexes in yeast (65, 66) as well as in a complex with the histone acetyltransferase TIP60 in human cells (67, 68).

We also identified several proteins with unknown function. The presence of KIAA1018 appears to be highly significant because of the extensive sequence coverage of this polypeptide in the MS analysis of the complexes bound to MLH1, PMS2, and PMS1 (see below). KIAA1018 appears to be identical to the MTMR15 (myotubularin-related protein 15). The MTMR proteins are characterized primarily by a tyrosine phosphatase domain and have been implicated in phosphoinositide metabolism, cellular growth, and differentiation. They were also found to be mutated in human genetic diseases (69). Most interestingly, the KIAA1018 protein was recently predicted to contain a RAD18-like zinc finger domain and to possess an endonuclease activity, which led to the suggestion that it may be involved in genome stability and maintenance (70).

Above, we described the use of TAP technology to identify interacting partners of the MMR proteins MLH1 and PMS2. This technique proved to be a valuable tool that allowed us to validate known interactions and to discover new potential binding partners of these important MutL homologues. The biological significance of the identified interactions will be evaluated for a selection of potentially interesting molecules that will hopefully help us to better understand the MMR mechanism and/or to discover novel functions of MutLα in the cell.

Identification of PMS1 Interacting Partners by Co-immunoprecipitation—As discussed above, PMS1 is one of the primary interacting partners of MLH1, as judged from the results of the TAP-MLH1 experiments (Table 1 and Fig. 3, *A* and *C*), yet it appears to lack a biological function. We set out to identify additional interacting partners of PMS1 in the hope that they might point us to the biological function of the stable and abundant heterodimer MutLβ. In this case, we decided against the TAP approach for two reasons. First, no human cell lines lacking PMS1 have been identified to date, which raised the possibility that the tagged polypeptide might compete with the untagged endogenous protein in the cell. Second, we do not have a functional assay that could be used to test whether the tag impairs the biological activity of PMS1. We therefore chose to deploy large scale co-immunoprecipitation coupled with MS analysis.

We immunoprecipitated PMS1 from 10 mg of HeLa whole cell extract, using an affinity-purified anti-PMS1 antibody. The purified preimmune serum was used as the negative control. The PMS1 antibody efficiently precipitated PMS1 and its major partner MLH1 from whole cell extracts, whereas the preimmune serum failed to do so (Fig. 4*A*). The immunoprecipitates were therefore separated by SDS-PAGE, the bands were visualized by Coomassie Blue staining (Fig. 4*B*), and the sample lane was cut into 15 slices. Following an in-gel tryptic digest, the eluted peptides were analyzed by MS as described above. We could identify a high number of novel PMS1-specific interacting partners, a subset of which was divided into functional categories (Table 3).

The analysis identified several potentially interesting molecules, but our attention was drawn to the presence of numerous proteins belonging to the ubiquitylation pathway and in particular to the ubiquitin-ligase EDD1, which was detected with a

very high Mascot score. This suggested that PMS1 might be post-translationally modified by ubiquitin. Our preliminary data show that this may indeed be the case. We transiently expressed hemagglutinin-tagged ubiquitin (HA-Ubi) in 293 cells and showed that it was expressed in high amounts (Fig. 4*C*, *left*). Immunoprecipitation with an anti-PMS1 antibody, followed by Western blot with an anti-HA tag antibody, revealed a strong signal in the HA-Ubi-transfected extracts (Fig. 4*C*, *center*). Reblotting with an anti-ubiquitin antibody suggested that a substantial proportion of the latter signal was due to endogenous polyubiquitylated PMS1 (Fig. 4*C*, *right*). However, the presence in the immunoprecipitate of deubiquitylating enzymes, such as UBP5, suggests that ubiquitylation of PMS1 may be a reversible process. Thus, it is conceivable that the biological role of the MutLβ heterodimer is modulated by ubiquitylation. This could take the form of an active participation in an as yet unidentified process of DNA metabolism. Alternatively, the polyubiquitylation may merely target PMS1 for proteasome-mediated degradation. We find the latter scenario particularly attractive, since controlled degradation of PMS1 would make more MLH1 available for heterodimerization with its other, catalytically active interaction partners PMS2 and MLH3. In this way, processes of DNA metabolism that rely on the latter heterodimers could be regulated without the need for transcriptional control.

DISCUSSION

Recent literature contains numerous examples documenting the involvement of MMR proteins in processes other than mismatch repair (1). We argued that identification of novel interacting partners of the MMR proteins, and the MutL homologues in particular, might provide us with important insights into the biological roles of these proteins outside of MMR. We opted for the TAP strategy, which has been successfully used in the characterization of protein complexes first in *S. cerevisiae* (28), but more recently also in other organisms, including human cells. Several studies compared TAP with single-tag purification strategies and immunoprecipitation experiments. TAP was shown to be significantly more specific, yielding fewer false positives (30). In *S. cerevisiae*, where large data sets are already available, the error rate of the TAP tag method has been estimated at about 15%, whereas for a single-epitope tag method, the error rate was about 50% (71). In addition, TAP uses mild washing conditions, allowing thus the recovery of native complexes. When performing TAP, the expression level of the tagged protein is an important determinant of the outcome of the experiment. For this reason, it is preferable to avoid the use of extracts from transiently transfected cells, where the expression levels of the tagged proteins are often extremely high. This may result in the identification of nonspecific interactors that bind to the overexpressed or misfolded protein. It may also make the identification of low abundant binding partners more difficult. The use of stably transfected cell lines allows for the selection of clones expressing the tagged protein at levels comparable with wild type.

One complication of the TAP strategy is that endogenous proteins might compete for binding partners with the stably expressed tagged protein, reducing thus the recovery of its interactors. To avoid this problem, it is preferable to stably transfect a cell line that lacks the target protein. This approach also enables testing the activity of the tagged protein in cell extracts, providing that an appropriate assay is available. In this study, we used MLH1-deficient 293T cells (34) for transfection with TAP-tagged MLH1 and PMS2-deficient HeLa12 cells (35) for transfection with TAP-tagged PMS2. TAP was then performed using whole cell extracts from the newly generated cell lines and, as negative control, from the parental, untransfected cells. The validity of the approach was confirmed by the fact that we were able to identify the majority of the known interacting partners of the MutL homologues in the eluted fractions but not in the controls. This gave us confidence that the novel interactions we detected are specific.

The interaction with angiomotin is a case in point. When the binding of MLH1 to Amot was detected, the protein was known only as an 80-kDa polypeptide (47). We identified an interaction with a ~130-kDa form, which was described only several months later (48). Our data thus showed that the specific interaction must be mediated by the 50-kDa N-terminal domain. Indeed, in pull-down experiments, only the larger

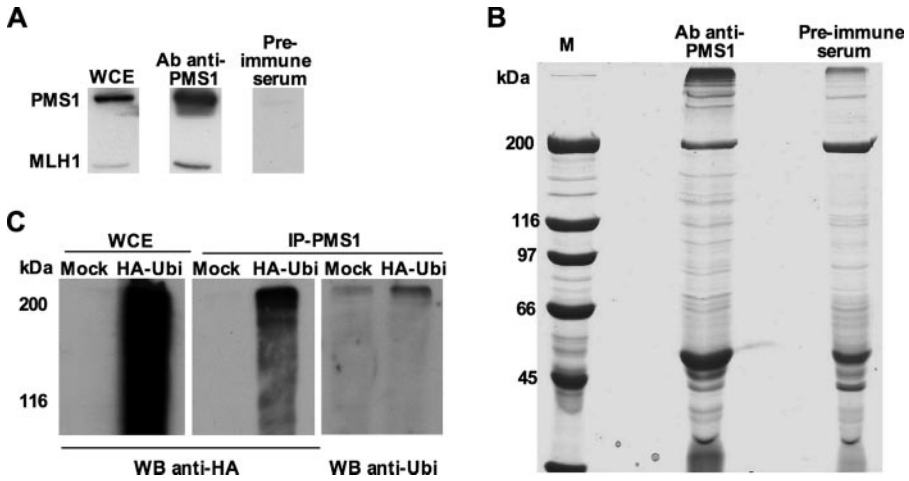

FIGURE 4. **Co-immunoprecipitation of PMS1-interacting partners from HeLa cell extracts.** *A*, Western blot analysis of PMS1 immunoprecipitates. Only the purified anti-PMS1 antibody and not the preimmune serum efficiently immunoprecipitated PMS1 and MLH1. *B*, example of large scale co-immunoprecipitation analysis of PMS1. The experiment was performed with 5 mg of whole cell extract and 1 μg of affinity-purified anti-PMS1 rabbit polyclonal antibody or purified preimmune serum. The immunoprecipitates were analyzed by SDS-PAGE and visualized by Coomassie staining. *M*, molecular size marker (2 μg/band). *C*, 1 mg of whole cell extract from 293 cells either mock-transfected (*Mock*) or transfected with a plasmid encoding HA-Ubi was incubated with an anti-PMS1 antibody. The immunoprecipitates (*IP-PMS1*) and the whole cell extracts (*WCE*) were analyzed by Western blot using an anti-HA tag antibody (*left* and *center*) or an anti-ubiquitin antibody (*right*). The smear observed on the HA-Ubi-transfected sample indicates the presence of poly-HA-ubiquitinated PMS1 (*center*). Incubation of the membrane with an anti-ubiquitin antibody resulted in a band at high molecular weight that indicated endogenous polyubiquitinated PMS1 in both mock-transfected and HA-ubiquitin-transfected cells.

protein specifically bound to MLH1 (Fig. 3*D*). Although there is little doubt that the two proteins interact, the biological significance of this interaction is not apparent. The 130-kDa isoform of Amot localizes to the cytoplasm and associates with actin fibers in endothelial cells; it was postulated to be involved in the change of cell morphology during tubulogenesis (48). The role of the 130-kDa isoform in epithelial cells is unexplored to date. Assuming that the interaction of Amot 130 with actin fibers is maintained also in epithelial cells, it will be of interest to test whether cellular morphology is affected by the absence of MLH1 or PMS2. It is also possible that the interaction may play a role in the nucleus; there is an emerging link between chromatin remodeling and polarity-determining proteins, and several tight junction proteins have been reported to regulate transcription of cell cycle-specific genes (72).

Mutations in the *BRCA1* gene are linked to breast cancer susceptibility. The protein has been implicated in the maintenance of genomic instability, although its molecular mechanism of action remains enigmatic. BRCA1 interacts with BRCA1-associated RING domain 1 (73) and BRIP1 (56) as well as with several other proteins involved in DNA metabolism, MLH1 among them (42). Our data now show that the latter interaction is most likely mediated via BRIP1 (Fig. 3*E*). It will be important to establish whether BRIP1 plays a role in MMR as a 5′–3′ helicase or whether it mediates the link between MMR and recombination. As mentioned above, MutL homologues are implicated in both mitotic and meiotic recombination, so finding an interacting partner implicated in recombination represents a direct confirmation of this involvement (2, 24). It is hoped that the identification of the MutLα-BRIP1-BRCA1 interaction will help shed new light on the molecular roles of these polypeptides in the maintenance of genomic stability.

The link of the MutL homologues with recombination was further underscored by the identification of KIAA1018. This polypeptide of unknown function has been assigned through sequence homology to the family of myotubularins and is tentatively denominated MTMR15. However, its bacterial and phage homologues have been shown to associate with a family of ATP-dependent recombinases that bind DNA and facilitate strand exchange. Moreover, BLAST homology searches identified a similarity with an archaeal Holliday junction resolvase (70).

The analysis of the interactome of the human MutL homologues MLH1, PMS1, and PMS2 identified several previously unidentified partners of this important class of proteins. Several of these interactions confirm the involvement of the MutL homologues in recombination observed in genetic studies many years ago. It could be speculated that the MutL complexes with BRIP1 and KIAA1018, as well as with the RuvB-like proteins, might function in branch migration and Holliday junction resolution. Whereas the interaction of the recombinogenic machinery with MMR was anticipated, the link with Amot was totally unexpected. However, this interaction could prove to be of substantial interest, especially if the complex can be linked to chromatin remodeling; the mammalian MMR protein MSH6 has at its N terminus a PWWP domain (74), which has been predicted to be involved in interactions with chromatin.

The human MMR system has recently been reconstituted from its purified recombinant constituents (5). Our present study provides biochemical evidence implicating the MMR proteins, and in particular the MutL homologues, in processes that go much beyond the repair of replication errors. We hope that the experiments described above will open new doors, which will lead to the full characterization of the biological roles and networks involving the MMR proteins and possibly also to a better understanding of their role in human cancer.

It is important to remember, however, that many protein-protein interactions detected in high throughput studies such as this may not be functionally relevant. It is possible that proteins interacting in a cell extract may not interact *in vivo*, because they may be confined to different cellular compartments or be expressed during different stages of the cell cycle. The biological relevance of protein-protein interactions must therefore be substantiated by functional studies, both *in vitro* and *in vivo*. Several of these are currently in progress in our laboratory.

Acknowledgments—We are grateful to Katja Baerenfaller and Torsten Kleffmann for help during the initial stages of this work, to Petr Cejka for helpful discussions and critical comments on the manuscript, to Elisabetta Pani and Mahmoud El-Shemerly for assistance with the fluorescence-activated cell sorting analyses and the ubiquitylation experiments, and Christine Hemmerle and Ritva Haider for technical assistance.

REFERENCES

1. Jiricny, J. (2006) *Nat. Rev. Mol. Cell. Biol.* **7,** 335–346
2. Hoffmann, E. R., and Borts, R. H. (2004) *Cytogenet. Genome Res.* **107,** 232–248
3. Modrich, P., and Lahue, R. (1996) *Annu. Rev. Biochem.* **65,** 101–133
4. Schär, P., and Jiricny, J. (1998) in *Nucleic Acids and Molecular Biology* (Eckstein, F., and Lilley, D. M. J., eds) Vol. 12, pp. 199–247, Springer Verlag, Berlin
5. Dzantiev, L., Constantin, N., Genschel, J., Iyer, R. R., Burgers, P. M., and Modrich, P. (2004) *Mol. Cell* **15,** 31–41
6. Zhang, Y., Yuan, F., Presnell, S. R., Tian, K., Gao, Y., Tomkinson, A. E., Gu, L., and Li, G. M. (2005) *Cell* **122,** 693–705
7. Palombo, F., Gallinari, P., Iaccarino, I., Lettieri, T., Hughes, M., D'Arrigo, A., Truong, O., Hsuan, J. J., and Jiricny, J. (1995) *Science* **268,** 1912–1914
8. Drummond, J. T., Li, G. M., Longley, M. J., and Modrich, P. (1995) *Science* **268,** 1909–1912
9. Palombo, F., Iaccarino, I., Nakajima, E., Ikejima, M., Shimada, T., and Jiricny, J. (1996) *Curr. Biol.* **6,** 1181–1184
10. Li, G. M., and Modrich, P. (1995) *Proc. Natl. Acad. Sci. U. S. A.* **92,** 1950–1954
11. Kunkel, T. A., and Erie, D. A. (2005) *Annu. Rev. Biochem.* **74,** 681–710
12. Raschle, M., Dufner, P., Marra, G., and Jiricny, J. (2002) *J. Biol. Chem.* **277,** 21810–21820
13. Jiricny, J. (2006) *Cell* **126,** 239–241
14. Kadyrov, F. A., Dzantiev, L., Constantin, N., and Modrich, P. (2006) *Cell* **126,** 297–308
15. Raschle, M., Marra, G., Nystrom-Lahti, M., Schar, P., and Jiricny, J. (1999) *J. Biol. Chem.* **274,** 32368–32375
16. Cannavo, E., Marra, G., Sabates-Bellver, J., Menigatti, M., Lipkin, S. M., Fischer, F., Cejka, P., and Jiricny, J. (2005) *Cancer Res.* **65,** 10759–10766
17. Prolla, T. A., Baker, S. M., Harris, A. C., Tsao, J. L., Yao, X., Bronner, C. E., Zheng, B., Gordon, M., Reneker, J., Arnheim, N., Shibata, D., Bradley, A., and Liskay, R. M. (1998) *Nat. Genet.* **18,** 276–279
18. Chen, P. C., Dudley, S., Hagen, W., Dizon, D., Paxton, L., Reichow, D., Yoon, S. R., Yang, K., Arnheim, N., Liskay, R. M., and Lipkin, S. M. (2005) *Cancer Res.* **65,** 8662–8670

19. de Wind, N., Dekker, M., Berns, A., Radman, M., and te Riele, H. (1995) *Cell* **82,** 321–330
20. de Wind, N., Dekker, M., Claij, N., Jansen, L., van Klink, Y., Radman, M., Riggins, G., van der Valk, M., van't Wout, K., and te Riele, H. (1999) *Nat. Genet.* **23,** 359–362
21. Baker, S. M., Plug, A. W., Prolla, T. A., Bronner, C. E., Harris, A. C., Yao, X., Christie, D. M., Monell, C., Arnheim, N., Bradley, A., Ashley, T., and Liskay, R. M. (1996) *Nat. Genet.* **13,** 336–342
22. Lipkin, S. M., Moens, P. B., Wang, V., Lenzi, M., Shanmugarajah, D., Gilgeous, A., Thomas, J., Cheng, J., Touchman, J. W., Green, E. D., Schwartzberg, P., Collins, F. S., and Cohen, P. E. (2002) *Nat. Genet.* **31,** 385–390
23. Baker, S. M., Bronner, C. E., Zhang, L., Plug, A. W., Robatzek, M., Warren, G., Elliott, E. A., Yu, J., Ashley, T., Arnheim, N., Flavell, R. A., and Liskay, R. M. (1995) *Cell* **82,** 309–319
24. Wei, K., Kuchelapati, R., and Edelmann, W. (2002) *Trends Mol. Med.* **8,** 346–353
25. Sugawara, N., Goldfarb, T., Studamire, B., Alani, E., and Haber, J. E. (2004) *Proc. Natl. Acad. Sci. U. S. A.* **101,** 9315–9320
26. Neuberger, M. S., Di Noia, J. M., Beale, R. C., Williams, G. T., Yang, Z., and Rada, C. (2005) *Nat. Rev. Immunol.* **5,** 171–178
27. Owen, B. A., Yang, Z., Lai, M., Gajek, M., Badger, J. D., II, Hayes, J. J., Edelmann, W., Kucherlapati, R., Wilson, T. M., and McMurray, C. T. (2005) *Nat. Struct. Mol. Biol.* **12,** 663–670
28. Rigaut, G., Shevchenko, A., Rutz, B., Wilm, M., Mann, M., and Seraphin, B. (1999) *Nat. Biotechnol.* **17,** 1030–1032
29. Puig, O., Caspary, F., Rigaut, G., Rutz, B., Bouveret, E., Bragado-Nilsson, E., Wilm, M., and Seraphin, B. (2001) *Methods* **24,** 218–229
30. Gingras, A. C., Aebersold, R., and Raught, B. (2005) *J. Physiol.* **563,** 11–21
31. Cejka, P., Stojic, L., Mojas, N., Russell, A. M., Heinimann, K., Cannavo, E., di Pietro, M., Marra, G., and Jiricny, J. (2003) *EMBO J.* **22,** 2245–2254
32. El-Shemerly, M., Janscak, P., Hess, D., Jiricny, J., and Ferrari, S. (2005) *Cancer Res.* **65,** 3604–3609
33. Perkins, D. N., Pappin, D. J., Creasy, D. M., and Cottrell, J. S. (1999) *Electrophoresis* **20,** 3551–3567
34. Trojan, J., Zeuzem, S., Randolph, A., Hemmerle, C., Brieger, A., Raedle, J., Plotz, G., Jiricny, J., and Marra, G. (2002) *Gastroenterology* **122,** 211–219
35. Ciotta, C., Ceccotti, S., Aquilina, G., Humbert, O., Palombo, F., Jiricny, J., and Bignami, M. (1998) *J. Mol. Biol.* **276,** 705–719
36. Stojic, L., Mojas, N., Cejka, P., Di Pietro, M., Ferrari, S., Marra, G., and Jiricny, J. (2004) *Genes Dev.* **18,** 1331–1344
37. Kondo, E., Horii, A., and Fukushige, S. (2001) *Nucleic Acids Res.* **29,** 1695–1702
38. Nielsen, F. C., Jager, A. C., Lutzen, A., Bundgaard, J. R., and Rasmussen, L. J. (2004) *Oncogene* **23,** 1457–1468
39. Schmutte, C., Sadoff, M. M., Shim, K. S., Acharya, S., and Fishel, R. (2001) *J. Biol. Chem.* **276,** 33011–33018
40. Umar, A., Buermeyer, A. B., Simon, J. A., Thomas, D. C., Clark, A. B., Liskay, R. M., and Kunkel, T. A. (1996) *Cell* **87,** 65–73
41. Gu, L., Hong, Y., McCulloch, S., Watanabe, H., and Li, G. M. (1998) *Nucleic Acids Res.* **26,** 1173–1178
42. Wang, Y., Cortez, D., Yazdi, P., Neff, N., Elledge, S. J., and Qin, J. (2000) *Genes Dev.* **14,** 927–939
43. Yazdi, P. T., Wang, Y., Zhao, S., Patel, N., Lee, E. Y., and Qin, J. (2002) *Genes Dev.* **16,** 571–582
44. Pedrazzi, G., Perrera, C., Blaser, H., Kuster, P., Marra, G., Davies, S. L., Ryu, G. H., Freire, R., Hickson, I. D., Jiricny, J., and Stagljar, I. (2001) *Nucleic Acids Res.* **29,** 4378–4386
45. Her, C., Vo, A. T., and Wu, X. (2002) *DNA Repair* (*Amst.*) **1,** 719–729
46. Bellacosa, A., Cicchillitti, L., Schepis, F., Riccio, A., Yeung, A. T., Matsumoto, Y., Golemis, E. A., Genuardi, M., and Neri, G. (1999) *Proc. Natl. Acad. Sci. U. S. A.* **96,** 3969–3974
47. Troyanovsky, B., Levchenko, T., Mansson, G., Matvijenko, O., and Holmgren, L. (2001) *J. Cell Biol.* **152,** 1247–1254
48. Ernkvist, M., Aase, K., Ukomadu, C., Wohlschlegel, J., Blackman, R., Veitonmaki, N., Bratt, A., Dutta, A., and Holmgren, L. (2006) *FEBS J.* **273,** 2000–2011
49. Bratt, A., Birot, O., Sinha, I., Veitonmaki, N., Aase, K., Ernkvist, M., and Holmgren, L. (2005) *J. Biol. Chem.* **280,** 34859–34869
50. Wu, X., Platt, J. L., and Cascalho, M. (2003) *Mol. Cell. Biol.* **23,** 3320–3328
51. Brieger, A., Plotz, G., Raedle, J., Weber, N., Baum, W., Caspary, W. F., Zeuzem, S., and Trojan, J. (2005) *Mol. Carcinog.* **43,** 51–58
52. Goldfarb, D. S., Corbett, A. H., Mason, D. A., Harreman, M. T., and Adam, S. A. (2004) *Trends Cell Biol.* **14,** 505–514
53. Levitus, M., Waisfisz, Q., Godthelp, B. C., de Vries, Y., Hussain, S., Wiegant, W. W., Elghalbzouri-Maghrani, E., Steltenpool, J., Rooimans, M. A., Pals, G., Arwert, F., Mathew, C. G., Zdzienicka, M. Z., Hiom, K., De Winter, J. P., and Joenje, H. (2005) *Nat. Genet.* **37,** 934–935
54. Levran, O., Attwooll, C., Henry, R. T., Milton, K. L., Neveling, K., Rio, P., Batish, S. D., Kalb, R., Velleuer, E., Barral, S., Ott, J., Petrini, J., Schindler, D., Hanenberg, H., and Auerbach, A. D. (2005) *Nat. Genet.* **37,** 931–933
55. Litman, R., Peng, M., Jin, Z., Zhang, F., Zhang, J., Powell, S., Andreassen, P. R., and Cantor, S. B. (2005) *Cancer Cell* **8,** 255–265
56. Cantor, S. B., Bell, D. W., Ganesan, S., Kass, E. M., Drapkin, R., Grossman, S., Wahrer, D. C., Sgroi, D. C., Lane, W. S., Haber, D. A., and Livingston, D. M. (2001) *Cell* **105,** 149–160
57. Park, J., Wood, M. A., and Cole, M. D. (2002) *Mol. Cell. Biol.* **22,** 1307–1316
58. Khavari, P. A., Peterson, C. L., Tamkun, J. W., Mendel, D. B., and Crabtree, G. R. (1993) *Nature* **366,** 170–174
59. Bochar, D. A., Wang, L., Beniya, H., Kinev, A., Xue, Y., Lane, W. S., Wang, W., Kashanchi, F., and Shiekhattar, R. (2000) *Cell* **102,** 257–265
60. Bauer, A., Chauvet, S., Huber, O., Usseglio, F., Rothbacher, U., Aragnol, D., Kemler, R., and Pradel, J. (2000) *EMBO J.* **19,** 6121–6130
61. Cho, S. G., Bhoumik, A., Broday, L., Ivanov, V., Rosenstein, B., and Ronai, Z. (2001) *Mol. Cell. Biol.* **21,** 8398–8413
62. Dugan, K. A., Wood, M. A., and Cole, M. D. (2002) *Oncogene* **21,** 5835–5843
63. Wood, M. A., McMahon, S. B., and Cole, M. D. (2000) *Mol. Cell* **5,** 321–330
64. Feng, Y., Lee, N., and Fearon, E. R. (2003) *Cancer Res.* **63,** 8726–8734
65. Shen, X., Mizuguchi, G., Hamiche, A., and Wu, C. (2000) *Nature* **406,** 541–544
66. Jonsson, Z. O., Jha, S., Wohlschlegel, J. A., and Dutta, A. (2004) *Mol. Cell* **16,** 465–477
67. Ikura, T., Ogryzko, V. V., Grigoriev, M., Groisman, R., Wang, J., Horikoshi, M., Scully, R., Qin, J., and Nakatani, Y. (2000) *Cell* **102,** 463–473
68. Frank, S. R., Parisi, T., Taubert, S., Fernandez, P., Fuchs, M., Chan, H. M., Livingston, D. M., and Amati, B. (2003) *EMBO Rep.* **4,** 575–580
69. Tronchere, H., Buj-Bello, A., Mandel, J. L., and Payrastre, B. (2003) *Cell Mol. Life Sci.* **60,** 2084–2099
70. Kinch, L. N., Ginalski, K., Rychlewski, L., and Grishin, N. V. (2005) *Nucleic Acids Res.* **33,** 3598–3605
71. Dziembowski, A., and Seraphin, B. (2004) *FEBS Lett.* **556,** 1–6
72. Sourisseau, T., Georgiadis, A., Tsapara, A., Ali, R. R., Pestell, R., Matter, K., and Balda, M. S. (2006) *Mol. Cell. Biol.* **26,** 2387–2398
73. Irminger-Finger, I., and Jefford, C. E. (2006) *Nat. Rev. Cancer* **6,** 382–391
74. Garcia, V., Salanoubat, M., Choisne, N., and Tissier, A. (2000) *Nucleic Acids Res.* **28,** 1692–1699

Characterization of the Interactome of the Human MutL Homologues MLH1, PMS1, and PMS2

Elda Cannavo, Bertran Gerrits, Giancarlo Marra, Ralph Schlapbach and Josef Jiricny

J. Biol. Chem. 2007, 282:2976-2986.
doi: 10.1074/jbc.M609989200 originally published online December 4, 2006
